The influence of magnetic nanoparticle concentration with dextran polymers in agar gel on heating efficiency in magnetic hyperthermia

Andrzej Skumiel [a],*, Katarzyna Kaczmarek [a], Dorota Flak [b], Michal Rajnak [c], Iryna Antal [c], Hubert Brząkała [a]

[a] Faculty of Physics, Adam Mickiewicz University, Uniwersytetu Poznańskiego 2, 61-614 Poznań, Poland
[b] NanoBioMedical Centre, Adam Mickiewicz University, Wszechnicy Piastowskiej 3, 61-614 Poznań, Poland
[c] Institute of Experimental Physics, Slovak Academy of Sciences, Watsonova 47, Košice 040 01, Slovakia

ABSTRACT

The article presents the results of research on the effect of magnetic hyperthermia performed on agar gel samples containing magnetite nanoparticles coated with dextran polymers for different molar weight M (150 kDa, 70 kDa, and 40 kDa). Regardless of the difference in molar dextran weights, these samples differed in a mass concentration of nanoparticles in the ferrogel C_0 (1.602 mg/cm^3, 2.506 mg/cm^3, 3.311 mg/cm^3, and 4.218 mg/cm^3). In the case of the highest magnetic field value H (20 kA·m^{-1}), the specific loss power SPL reaches 70 W·g^{-1} for nanoparticles with 150 kDa dextran at a concentration of nanoparticles $C_0 = 1.602$ mg/cm^3. An oscillating magnetic field with an amplitude up to 20 kA·m^{-1} and a frequency of 357 kHz was used in the study.

© 2020 The Authors. Published by Elsevier B.V. This is an open access article under the CC BY license (http://creativecommons.org/licenses/by/4.0/).

1. Introduction

The use of magnetic nanoparticles in medicine is well known in magnetic hyperthermia treatments for the destruction of an oncological tumor. In this case, magnetite nanoparticles with a diameter of several nanometers are introduced into the tumor and an oscillating magnetic field with a frequency of several hundred kilohertz is applied. Under the influence of this oscillating magnetic field [1–4], nanoparticles become a source of heat emitted in diseased tissues. In recent years, attempts have also been made to use a rotating magnetic field in magnetic hyperthermia to stimulate magnetic nanoparticles [5–8]. According to the authors of the article [5], experiments with a rotating magnetic field show up to 2–3 times higher thermal efficiency compared to a 1-axis oscillating field. Recently, we have encountered further attempts to increase the hyperthermia effect through the simultaneous application of an alternating magnetic field and an ultrasonic wave at a frequency of 1–3 MHz, which can easily be focused in the desired place of the body [9,10]. An additional advantage of using ultrasound, in this case, is the ability to control and monitor the process temperature. In clinical practice, the tumor area with cancerous cells reaches a temperature of about 42–43 °C, which is several degrees higher than the body's physiological temperature. These diseased cancer cells are less resistant to overheating than healthy cells and are then destroyed.

On the one hand, the amount of heat released during magnetic hyperthermia is influenced by the parameters of the magnetic field (amplitude of the intensity H and frequency of the magnetic field f), but on the other hand by the type and structure of nanoparticles with the surfactant layer, their concentration, as well as the properties of the medium in which they are suspended. Various thermal effects occur when nanoparticles are suspended in a magnetic liquid with a low viscosity coefficient, others when they are in an agar gel, and others when they are in a living organism [16]. In the case of magnetic hyperthermia carried out in vivo, blood flow through the heating area weakens the heating effect. The studies described in this article were made with Fe_3O_4 magnetite nanoparticles, with polymer dextran as a surfactant of various molecular weight and were suspended in agar gel. Due to the similar properties of the agar gel to the soft tissues of the body, the conditions of the in vitro experiment are similar to in vivo [17,18].

2. Experimental methods and results

2.1. Construction and parameters of magnetic circuits

Experimental studies of magnetic hyperthermia were carried out in a variable magnetic field. The measuring system was developed by EASYHEAT (Ambrell Corporation, Scottsville, NY, United States, model: 1.2 kW–2.4 kW Induction Heating Systems 0112 m 0224) which consisted of a coil connected in parallel with a high-voltage electric

* Corresponding author.
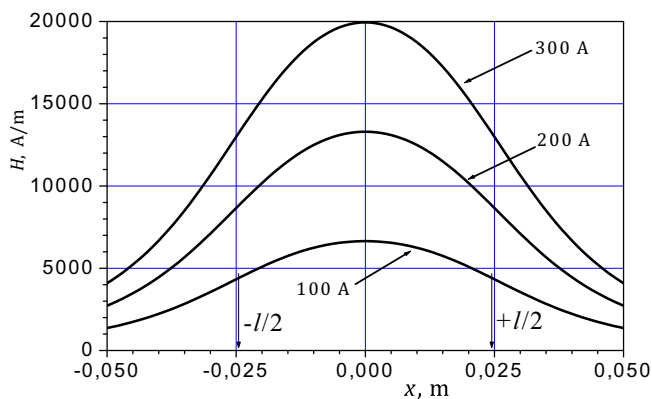E-mail address: skumiel@amu.edu.pl (A. Skumiel).

Fig. 1. The distribution of the magnetic field strength amplitude along the axis of the solenoid.
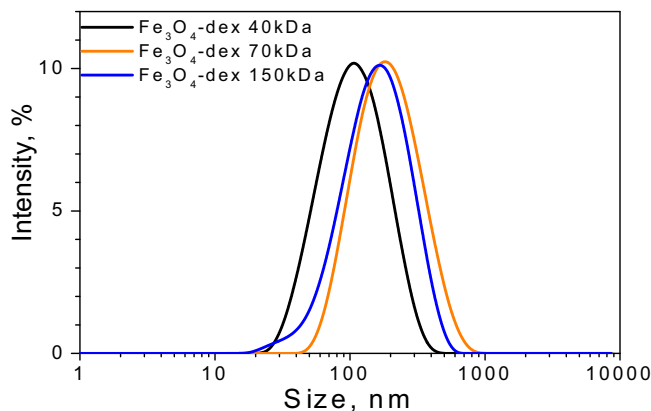

Fig. 2. Representative size distribution by the intensity of the hydrodynamic diameter of prepared magnetite nanoparticles coated with dextran (40, 70 and 150 kDa) measured by the dynamic light scattering (DLS).

capacitor, which meant that the electrical impedance (in the resonance of currents) of such an *LC* system was high and thus did not overload the generator too much. Because of the high current (up to 300 A) flowing through the coil, it was made of a thin-walled copper tube cooled by water flowed from the thermostatic system. During hyperthermia experiments, an agar gel containing magnetite nanoparticles was placed inside the coil.

Depending on the value of the set current *I* the amplitude of the magnetic field *H*(x) was calculated along the coil axis according to formula (1). The dependence (1) was obtained using the Biot-Savart law [11,12],

$$H_x = \frac{n \cdot I}{2l} \left(\frac{x + \frac{l}{2}}{\sqrt{R^2 + \left(x + \frac{l}{2}\right)^2}} - \frac{x - \frac{l}{2}}{\sqrt{R^2 + \left(x - \frac{l}{2}\right)^2}} \right) \quad (1)$$

where $R = 0.0285$ m, $l = 0.049$ m and $n = 5$ are the radius, the length and the number of turns of the coil respectively. The distance x is measured along the coil axis from its center. At the middle point of the coil (x = 0), there is the maximum intensity of the magnetic field.

$H_{(x=0)} = H_{max}$. Fig. 1 shows a graphical description of the relationship $H(x)$ for several selected currents $I = 100, 200$ and 300 A. In the central part of the coil, in this case, the magnetic field reached 6.7, 13.3 and 20 kA·m^{-1}.

2.2. Characteristics of magnetic fluid used for phantom preparation

For experimental studies dextran magnetic fluids (DEX-MFs) were prepared using the slightly modified Molday procedure [13]. Each liquid had a different molecular weight of dextran forming the nanoparticle surfactant layer and different mass concentrations of nanoparticles were used: 32 mg/cm^3, 44 mg/cm^3 and 46 mg/cm^3. The molecular weights M of dextran were $M = 70$ kDa for liquids of magnetic nanoparticles concentration equals to 32 mg·cm^{-3}, $M = 150$ kDa for liquids of concentration 44 mg·cm^{-3}, and $M = 40$ kDa for liquids of concentration 46 mg·cm^{-3}.

The particle size distribution of prepared magnetite nanoparticles coated with dextran of various lengths (40, 70 and 150 kDa) was measured on Zetasizer Nano-ZS (Malvern Instruments, Malvern, UK) with the non-invasive dynamic light scattering method (DLS-NIBS) using an angle of 173 at 25 °C. Values of a hydrodynamic diameter such as Z-average and size by intensity ($d_{Intensity}$), were obtained from the cumulative and the least-squares analysis of the recorded correlation function, respectively, along with the polydispersity index (PDI). As obtained dextran-coated Fe$_3$O$_4$ nanoparticles were diluted in deionized water (H$_2$O$_d$) prior to the measurement. Results are the mean ± standard deviation of three measurements on three individually prepared sample dilutions (each of three analyses). Summary of the results on the hydrodynamic particle size distribution of as-obtained Fe$_3$O$_4$ nanoparticles coated with dextran of various lengths is given in Table 1 and Fig. 2.

It is presented that dextran coating has a significant effect on the hydrodynamic particle size as compared with bare magnetite nanoparticles, and the use of different length dextran leads to the formation of nanoparticles with significantly different sizes and of low standard deviations. Dextran coating leads to the particles increase from ~10 nm to 119.2 nm, 212.0 nm and 175.9 nm for Fe$_3$O$_4$-dex 40 kDa, Fe$_3$O$_4$-dex 70 kDa and Fe$_3$O$_4$-dex 150 kDa, respectively. Surprisingly, the coating

Table 1
Summary of dynamic light scattering (DLS) measurements.

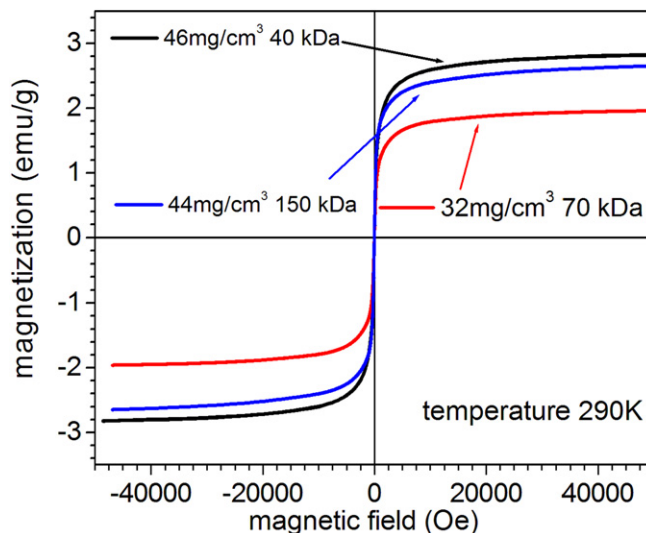| Sample	Z-average	$D_{intensity}$	PDI[a]
Fe$_3$O$_4$-dex 40 kDa	95.9 ± 2.1 nm	119.2 ± 7.8 nm	0.224 ± 0.029
Fe$_3$O$_4$-dex 70 kDa	162.1 ± 2.3 nm	212.0 ± 15.3 nm	0.233 ± 0.009
Fe$_3$O$_4$-dex 150 kDa	132.4 ± 5.6 nm	175.9 ± 10.1 nm	0.266 ± 0.041

[a] PDI – polydispersity index.

Fig. 3. Magnetization curves of magnetite liquids with molecular mass of dextran: $M = 40$, 70 and 150 kDa determined by the VSM method.

Table 2
Summary of vibrating sample magnetization (VSM) measurements.

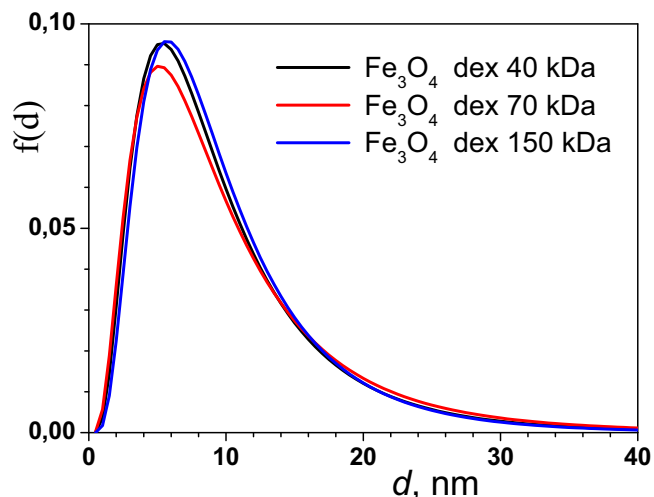| Sample	$\langle d \rangle$	σ	d_o	β
	nm	nm	nm	–
40 kDa	10.05	5.31	8.131	0.651
70 kDa	10.62	6.63	8.349	0.696
150 kDa	10.11	6.86	8.362	0.616

Fig. 4. Magnetic mean size distribution obtained from magnetization curves of magnetic fluids with molecular mass of dextran: $M = 40$, 70 and 150 kDa.

of the NPs with the highest length dextran of 150 kDa does not yield NPs with the largest size. NPs coated with medium dextran length of 70 kDa exhibit the largest particle size. All investigated samples have a medium range of polydispersity (PDI values within the range of 0.08–0.7), which makes them suitable for the foreseen application.

Magnetic measurements using a vibrating sample vibrometer (VSM) were performed to determine the size of the magnetite nanoparticles and to determine their distribution function. The magnetization curves are shown in Fig. 3 do not reveal magnetic hysteresis.

For the polydisperse system of nanoparticles present in the magnetic liquid, the lognormal distribution function (2a) is most often used in the form [1]:

$$f(d) = \frac{1}{\sqrt{2\pi}d\beta} \exp\left[\frac{-\left(\ln\frac{d}{d_o}\right)^2}{2\beta^2}\right],$$

(2a)

where d is the diameter, d_o and β are the parameters to be determined. Table 2 presents the mean diameters $\langle d \rangle$, the mean standard deviations

$\langle \sigma \rangle$ from $\langle d \rangle$ obtained by the VSM method. The following formulae were used:

$$\langle d \rangle = d_o \, exp\left(\frac{\beta^2}{2}\right) \text{ and } \sigma = \langle d \rangle \cdot \sqrt{exp\left(\beta^2\right) - 1}$$

(2b)

On the basis of the obtained parameters d_o and β the distribution functions of magnetite nanoparticles are shown in Fig. 4. In turn, Fig. 5 shows electron microscope images of the three samples of magnetic fluids, shown with the same magnification.

Measurements carried out by the DLS method indicate that the hydrodynamic diameters of nanoparticles ($d_{hyd} \geq 100$ nm) are at least one order larger than the size of the magnetic core determined by the VSM method ($\langle d \rangle \cong 10$ nm). This means that in this case, it dominates the relaxation mechanism of magnetization according to Néel [1]. TEM images also confirm that average magnetite diameter sizes are in the order of 10 nm.

2.3. Preparation of ferrogel samples and their physical properties

All gel samples prepared for testing had a volume of 1.42 cm^3 and the same agar concentration of 5%. The remaining 95% of the mass was water and magnetic liquid in proportions depending on the desired concentration of magnetite nanoparticles in a given sample (0.16%, 0.25%, 0.33%, 0.42%). Calculated as mg/cm^3, these mass concentrations were 1.602 mg/cm^3, 2.506 mg/cm^3, 3.311 mg/cm^3 and 4.218 mg/cm^3, respectively.

The entire ferrogel sample preparation process was carried out at room temperature. Appropriate amounts of ingredients, powdered agar, water, and magnetic liquid were weighed separately using an analytical balance. The measured amount of water was poured into a beaker with magnetic liquid, and then this solution was heated for several seconds in a microwave oven until boiling and poured into a beaker with powdered agar. Using a glass rod for about 20 s, the resulting mixture was manually mixed and then treated with an ultrasonic homogenizer for 15 s.

The homogeneous material thus obtained was allowed to cool for a few minutes. When the mixture in the beaker was already starting to solidify, it was poured into smaller 2.2 ml glass vials and left for 24 h for full gelation. After 24 h, the solid samples were cut to a height of 2 cm. Such agar phantoms had a volume of 1.42 cm^3 ($d = 0.95$ cm, $h = 2$ cm) and were tested in an alternating magnetic field. Because tissue-mimicking agar phantoms during a longer period of time can easily grow mold or shrink due to water evaporation, the measurements were carried out on fresh samples within 30 h of the start of the setting.

2.4. Calorimetric measurements

An optical fiber thermometer FISO Technologies Inc. with an accuracy of ± 0.1 °C was used to measure the temperature of the heated
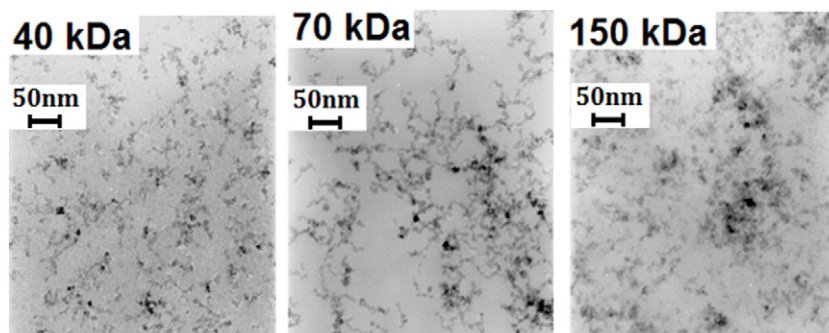

Fig. 5. TEM images of magnetite particles with different of molecular mass dextran.
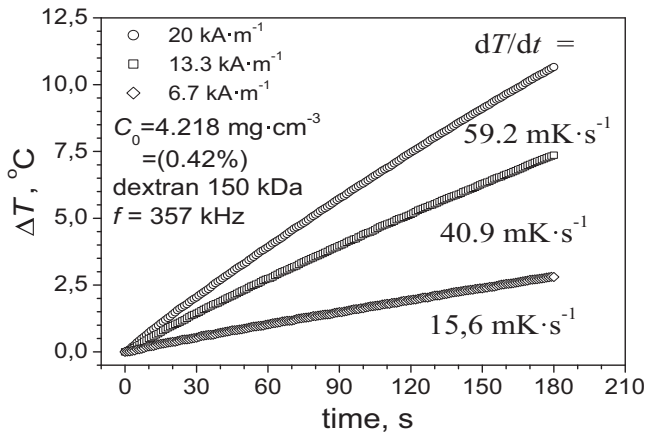
Fig. 6. Measured temperature increase *versus* time for various intensities of magnetic fields at frequency $f = 357$ kHz. Phantom agar sample – with dextran 150 kDa as surfactant – containing magnetic nanoparticles with a mass concentration of $C_0 = 4.218$ mg·cm^{-3}.

Table 3
Experimental values of the initial temperature increase rate (dT/dt) for different values of the magnetic field strength amplitude H of ferrogel agar samples with mass concentration of nanoparticles in the sample ($C_0 = 4.218$ mg·cm^{-3} and 1.603 mg·cm^{-3}) for different molecular weights M of dextran.

Mass concentration of nanoparticles in the sample C_0 [mg·cm^{-3}]	Dextran	H [kA·m^{-1}]		
		6.7	13.3	20
		dT/dt, mK·s^{-1}		
4.218	150 kDa	15.6	40.9	59.2
	70 kDa	8.2	18.1	26.7
	40 kDa	4.3	11.8	18.4
1.603	150 kDa	7.4	23.52	32.74
	70 kDa	5.17	10.21	14.07
	40 kDa	3.33	7.66	10.38

ferrogel sample. The temperature change of the pure agar gel caused by heating from the coil with the current was also checked. In the case of the strongest magnetic field, the change in temperature of the pure agar gel was slightly ten times less than compared to the gel containing magnetic nanoparticles.

When analyzing the results of the hyperthermia effect, the temperature change caused by heated solenoid was taken into account. In addition, in order to limit the impact of this additional effect, polystyrene was inserted between the sample and coil as a heat insulator. All magnetic hyperthermia measurements were taken at an ambient temperature of 25 °C and at frequency $f = 357$ kHz, with the magnetic field strength up to 20 kA/m.

In Fig. 6 as an example, the temperature change *vs.* time curves in a sample of agar ferrogel with magnetic particles at a concentration of 4.218 mg/cm^3 magnetite, coated with dextran with a molecular weight of 150 kDa, are presented. Samples of the measured temperature were recorded every 1 s. The recorded (during 180 s) temperature curves shown in Fig. 6, are almost linear, which indicates good thermal insulation of the samples.

In turn Table 3 presents the values of the temperature increase rate (dT/dt) for samples with different values of dextran molecular weight ($M = 40$ kDa, 70 kDa and 150 kDa), after 180 s from the application of a magnetic field with several chosen amplitudes for mass concentration of nanoparticles in the sample $C_0 = 4.218$ mg·cm^{-3} and 1.603 mg·cm^{-3}.

The experimental numerical values from Table 3 are also graphically illustrated in Fig. 7.

The obtained experimental results show that for the same concentration of magnetic nanoparticles in the ferrogel ($C_0 = 4.218$ mg·cm^{-3}), the rate of temperature rise (dT/dt) increases both with the increase in the magnetic field strength H and the molecular weight of the surfactant used (dextran).

3. Analysis

In the literature on magnetic hyperthermia, two parameters are often found that describes the efficiency of thermal energy released. One of them is the specific absorption rate SAR_{SAMPLE}, which determines the thermal power released in 1 g of the sample, for example in 1 g of tissue. In order to effectively heat the body soft tissues, it is assumed in the literature [4] that this coefficient should have a minimum value of 100 mW·g^{-1}.

Another parameter is the specific loss power (SLP), which allows assessing the amount of thermal power that is released by 1 g of magnetic material contained in a magnetic liquid, in a ferrogel or in the soft tissues of the body. Table 4 summarizes the temperature change ΔT recorded during temperature measurement and temperature increase rate dT/dt. The values listed in Table 4 were determined in a magnetic field with an intensity of $H = 20$ kA·m^{-1} and at frequency $f = 357$ kHz.

The temperature increase rate dT/dt shown in Fig. 8 indicates that at the same concentration of magnetitic nanoparticles in the ferrogel, more heat will be released for samples having a higher molecular weight of dextran ($M = 150$ kDa).

This can be explained by the fact that when the magnetic core is in a larger dextran envelope (lower dynamic viscosity coefficient than in gel), it has more freedom to rotate under the influence of an oscillating
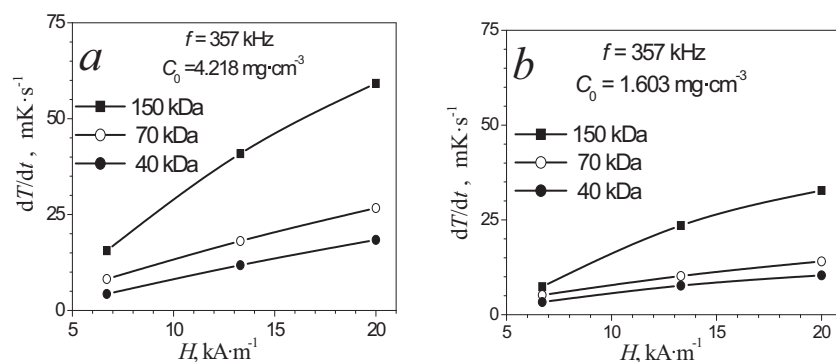

Fig. 7. The temperature increase rate (dT/dt) *versus* magnetic field strength amplitude H of ferrogel agar samples with mass concentration of nanoparticles in the sample (a) $C_0 = 4.218$ mg·cm^{-3} and (b) $C_0 = 1.603$ mg·cm^{-3} for different molecular weights M of dextran.

Table 4

The temperature change ΔT, the temperature increase rate dT/dt, the specific absorption rate SAR_{SAMPLE} and specific loss power SLP depending on mass concentration of nanoparticles in the ferrogel C_0 prepared on the basis of magnetic liquids with dextran polymers of different molecular weight ($M = 40$ kDa, 70 kDa and, 150 kDa) at maximum magnetic field $H = 20$ kA·m^{-1} at frequency $f = 357$ kHz.

Surfactant of magnetic particles (dextran polymers) M	C_0		ΔT	dT/dt	SLP
	%	mg·cm^{-3}	°C	mK·s^{-1}	W·g^{-1}
40 kDa 46 mg·cm^{-3}	0.16	1.603	1.75	9.7	25.4
	0.25	2.506	2.28	12.7	21,2
	0.33	3.311	2.97	16.5	20.9
	0.42	4.218	3.31	18.4	18.3
70 kDa 32 mg·cm^{-3}	0.16	1.603	2.38	13.2	34.5
	0.25	2.506	3.23	17.9	30.0
	0.33	3.311	3.80	21.1	26.7
	0.42	4.218	4.80	26.7	26.5
150 kDa 44 mg·cm^{-3}	0.16	1.603	4.88	27.1	70.8
	0.25	2.506	6.34	35.2	58.9
	0.33	3.311	7.87	43.7	55.4
	0.42	4.218	10.66	59.2	58.9

Table 5

Mass concentration C_0 of magnetic nanoparticles in ferrogel, volume V of nanoparticles in 1 cm^3 of ferrogel, number N of nanoparticles in 1 cm^3, and the distance L_x between the centers of nanoparticles uniformly distributed in 1 cm^3 of the sample.

C_0 [mg·cm^{-3}]	V [cm^3]	N -	L_x [nm]
1.603	3.09 · 10^{-4}	1.2 · 10^{14}	203
2.506	4.84 · 10^{-4}	1.88 · 10^{14}	175
3.311	6.39 · 10^{-4}	2.49 · 10^{14}	159
4.218	8.14 · 10^{-4}	3.17 · 10^{14}	147

magnetic field. In this case, it can also indicate that the heat was released by the Brown mechanism.

To determine the thermal power released by nanoparticles contained in phantoms with different mass concentration $C_0 = m_{NP}/m_S$, specific loss power (SLP) was determined by the formula [14,15]:

$$SLP = c_S \frac{m_S}{m_{NP}} \left(\frac{\Delta T}{\Delta t}\right) = \frac{C_S}{C_0} \cdot \left(\frac{\Delta T}{\Delta t}\right) \tag{3}$$

where c_s is the specific heat capacity of the phantom sample, $m_s \cong 1.42$ g is the phantom mass, and m_{NP} is the mass of the magnetite nanoparticles. In our the case value of the specific heat capacity is similar to water: $c_s \cong 4.18$ J·g^{-1} K^{-1}.

Fig. 9a indicates that for the concentrations of nanoparticles in the sample $C_0 < 3.311$ mg·cm^{-3}, the SLP parameter begins to increase for lower concentration values. The probable reason for this is the influence of interactions between neighboring magnetite nanoparticles at their higher concentrations in the sample.

Table 5 contains several parameters: V - volume, N - number of nanoparticles and L_x – the distance between the centers of nanoparticles, calculated for different concentrations of magnetite nanoparticles, assuming that they are distributed uniformly in phantom volume and do not form agglomerates.

The graphical relationship between the distance L_x and nanoparticles along the x-axis is shown in Fig. 9b. Distance L_x increases as the concentration C_0 decreases. Thus, at lower concentrations the distance L_x between nanoparticles increases, which means less interaction between nanoparticles. As a result, magnetic nanoparticles have greater freedom to vibrate under the influence of an alternating magnetic field and an increase of SLP parameter is observed at lower concentration values.

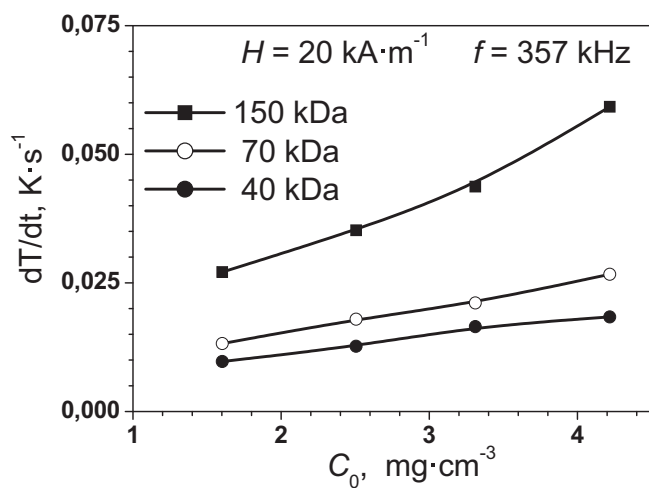**Fig. 8.** The initial temperature increase rate for different values of mass concentration C_0 of nanoparticles in the gel sample.

4. Conclusions

The obtained experimental results (Fig. 7a, 7b) show that at a constant concentration C_0 of magnetic nanoparticles in a ferrogel sample, the parameter (dT/dt) increases with the increase in the magnetic field strength H and the molecular mass M of the surfactant (dextran). Moreover, a comparison of dependencies presented in Fig. 7a, 7b shows that also the increase in the C_0 concentration of magnetic nanoparticles in the ferrogel sample leads to an increase in the dT/dt parameter.

Higher concentration C_0 of magnetic nanoparticles in the ferrogel sample causes a decrease in the distance between nanoparticles in the gel network (Fig. 9b) and thus increases the interactions between them.

When the nanoparticles are closer to each other (at smaller distances Lx) dipole-dipole interactions can deteriorate the heating efficiency of a sample [19]. Therefore for a higher concentration of nanoparticles lower values of specific loss power can be observed
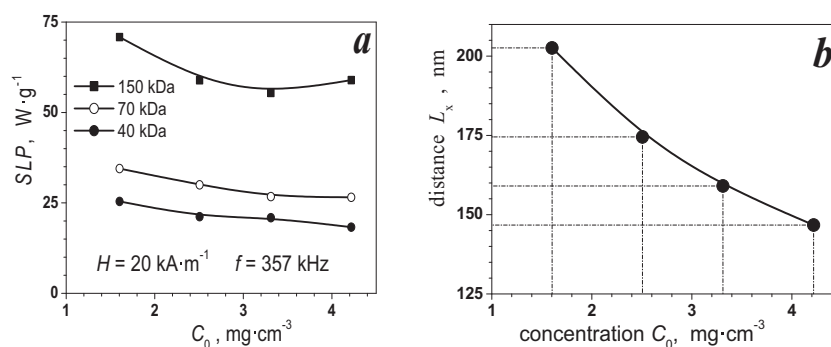

Fig. 9. The dependences of the specific loss power SLP – (a) for different values of mass concentration C_0 of nanoparticles in the sample and the dependences of distance L_x between the centers of nanoparticles uniformly distributed in the sample depending on the concentration C_0 (b).

(Fig. 9a). It can also be seen in Fig. 9a that at a given C_0 concentration, *SLP* increases with increasing molecular weight M of the surfactant.

Ferrogel structure can hinder Brown relaxation - deteriorate movement of magnetic nanoparticles comparing to easy movement of magnetic nanoparticles in ferrofluids. Therefore we assume that when the magnetic core is in a larger dextran envelope (lower dynamic viscosity coefficient than in gel), it gives more freedom to magnetic nanoparticles to rotate in gel structure which results in presented better heating efficiency for the higher molecular weight of dextran. Due to the large hydrodynamic diameters of nanoparticles compared to the size of magnetite grains, the Néel magnetizing mechanism is the dominant.

Declaration of competing interest

The article was created without a conflict of interest.

Acknowledgments

Contributions

(A. Skumiel): analysis of results, physical calculations, preparation of the manuscript and corresponding author; (K. Kaczmarek): student supervising, help in part of experimental research and co-author of the final version of the article; (Dorota Flak): measurements and description of DLS; (Michal Rajnak): magnetic measurements of magnetic fluids; (Iryna Antal): magnetic fluid synthesis. (H. Brząkała): performing hyperthermia measurements.

References

[1] R.E. Rosensweig, Heating magnetic fluid with alternating magnetic field, J. Magn. Magn. Mater. 252 (2002) 370–374.

[2] A. Skumiel, M. Kaczmarek-Klinowska, M. Timko, M. Molcan, M. Rajnak, Evaluation of power heat losses in multidomain Iron particles under the influence of AC magnetic field in RF range, Int. J. Thermophys. 34 (4) (2013) 655–666.

[3] A. Skumiel, A. Jozefczak, M. Timko, et al., Heating effect in biocompatible magnetic fluid, Int. J. Thermophys. 28 (5) (2007) 1461–1469.

[4] Q.A. Pankhurst, J. Connolly, S.K. Jones, J. Dobson, Applications of magnetic nanoparticlesin biomedicine, J. Phys. D. Appl. Phys. 36 (2003) R167–R181.

[5] V.A. Sharapova, M.A. Uimin, A.A. Mysik, A.E. Ermakov, Heat release in magnetic nanoparticles in AC magnetic fields, Phys. Met. Metallogr. 110 (1) (2010) 5–12.

[6] A. Skumiel, B. Leszczyński, M. Molcan, M. Timko, The comparison of magnetic circuits used in magnetic hyperthermia, J. Magn. Magn. Mater. 420 (2016) 177–184.

[7] M. Beković, et al., A comparison of the heating effect of magnetic fluid between the alternating and rotating magnetic field, J. Magn. Magn. Mater. 355 (2014) 12–17.

[8] A. Skumiel, A device for producing a high frequency rotating magnetic field, Patent No. PL230206, UPRP, (2018).

[9] A. Józefczak, K. Kaczmarek, T. Hornowski, M. Kubovcˇıkova, Z. Rozynek, M. Timko, A. Skumiel, Magnetic nanoparticles for enhancing the effectiveness of ultrasonic hyperthermia, Appl. Phys. Lett. 108 (2016), 263701.

[10] K. Kaczmarek, T. Hornowski, I. Antal, M. Rajnak, M. Timko, A. Józefczak, Sono-magnetic heating in tumor phantom, J. Magn. Magn. Mater. 500 (2020), 166396. https://doi.org/10.1016/j.jmmm.2020.166396.

[11] G. Dahake, Nanoparticle heating using induction in hyperthermia, ASM Handbook, Induction Heating and Heat Treatment, 800 Special Applications of Induction Heating, 4C, , 2014.

[12] R.M. Eisberg, L.S. Lerner, Physics, Foundations and Applications, The Biot-Savart Law, , McGraw-Hill Book Company, New York, 1981 1086–1096 Chapter 23-5.

[13] R.S. Molday, D. Mackenzie, Immunospecific ferromagnetic iron-dextran reagents for the labeling and magnetic separation of cells, J. Immunol. Methods 52 (3) (1982) 353–367.

[14] Shu-Yi Wang, et al., Potential sources of errors in measuring and evaluating the specific loss power of magnetic nanoparticles in an alternating magnetic fiels, IEEE Trans. Magn. 49 (1) (2013) 255–262.

[15] T.R. Oliveira, et al., Magnetic fluid hyperthermia for bladder cancer: a preclinical dosimetry study, Int. J. Hyperth. 29 (8) (2013) 835–844.

[16] K. Kaczmarek, R. Mrówczyński, T. Hornowski, R. Bielas, A. Józefczak, The effect of tissue-mimicking phantoms compressibility on magnetic hyperthermia, Nanomaterials 9 (2019) 803.

[17] A. Dabbagh, B.J.J. Abdullah, C. Ramasindarum, N.H. Abu Kasim, Tissue-mimicking gel phantoms for thermal therapy studies, Ultrason. Imaging 36 (4) (2014) 291–316.

[18] A. Józefczak, K. Kaczmarek, M. Kubovčíková, Z. Rozynek, T. Hornowski, The effect of magnetic nanoparticles on the acoustic properties of tissue-mimicking agar-gel phantoms, J. Magn. Magn. Mater. 431 (2017) 172–175.

[19] R. Fu, Y. Yan, C. Roberts, Z. Liu, Y. Chen, The role of dipole interactions in hyperthermia heating colloidal clusters of densely-packed superparamagnetic nanoparticles, Sci. Rep. 8 (2018) 4704.